

ELECTROCHEMISTRY OF STRESS CORROSION CRACKING OF  
TITANIUM ALLOYS IN CHLORIDE ENVIRONMENTS

A THESIS

Presented to

The Faculty of the Graduate Division

by

Roberto Piccinini

In Partial Fulfillment  
of the Requirements for the Degree  
Master of Science in Metallurgy

Georgia Institute of Technology

September, 1972



In presenting the dissertation as a partial fulfillment of the requirements for an advanced degree from the Georgia Institute of Technology, I agree that the Library of the Institute shall make it available for inspection and circulation in accordance with its regulations governing materials of this type. I agree that permission to copy from, or to publish from, this dissertation may be granted by the professor under whose direction it was written, or, in his absence, by the Dean of the Graduate Division when such copying or publication is solely for scholarly purposes and does not involve potential financial gain. It is understood that any copying from, or publication of, this dissertation which involves potential financial gain will not be allowed without written permission.

---

7/25/68



ELECTROCHEMISTRY OF STRESS CORROSION CRACKING OF  
TITANIUM ALLOYS IN CHLORIDE ENVIRONMENTS

Approved:

Robert F. Hochman, Chairman

Helen E. Grenga

Edgar A. Starke, Jr.

Date approved by Chairman:

8/11/72



## ACKNOWLEDGMENTS

The author wishes to express his deepest gratitude to Dr. Robert F. Hochman, his thesis advisor, for his continuous support, encouragement and patience during this work.

Great appreciation is extended to Dr. Miroslav Marek, for his invaluable help in the experimental procedure and in the discussion of the results.

A special note of thanks goes to Mr. Antoine Pourbaix of the Centre Belge d'Etude de la Corrosion CEBELCOR, Belgium, for his original ideas in devising the experimental technique.

The author is also grateful to Dr. Edgar A. Starke, Jr., and Dr. Helen E. Grenga for their review of this work.

The support by the Advanced Research Project Agency (ARPA Order No. 878) and the Atlantic Steel Company and the Texaco Fellowship in Metallurgy is acknowledged.



## TABLE OF CONTENTS

	Page
ACKNOWLEDGMENTS . . . . .	ii
LIST OF TABLES . . . . .	iv
LIST OF FIGURES . . . . .	v
SUMMARY . . . . .	vi
CHAPTER	
I. INTRODUCTION . . . . .	1
Stress Corrosion Cracking Characteristics	
Parameters Influencing Stress Corrosion Cracking	
Stress Corrosion Cracking Theories	
The Occluded Cell Corrosion	
II. EXPERIMENTAL PROCEDURE . . . . .	16
Potential-Load Experiments	
pH-Time Experiments	
III. DISCUSSION OF RESULTS . . . . .	25
Potential-Load Curves	
pH-Time Curves	
Hydrolysis Products	
Potential Measurements	
IV. CONCLUSIONS . . . . .	41
Potential-Load Experiments	
pH-Time Experiments	
V. RECOMMENDATIONS . . . . .	42
BIBLIOGRAPHY . . . . .	43



## LIST OF TABLES

Table		Page
1.	Analysis of the Titanium and Titanium-Aluminum Alloys Tested . . . . .	17
2.	Lowest pH Values Recorded for the Materials Tested . . . .	31
3.	"Incubation" Times for the Materials Tested . . . . .	32
4.	Possible Active Surface Reactions and Their Standard Potentials . . . . .	38



## LIST OF FIGURES

Figure		Page
1.	General View of the Potential-Load Testing Apparatus . . .	18
2.	Detail of the Potential-Load Cell . . . . .	19
3.	General View of the pH-Time Testing Apparatus . . . . .	20
4.	Details of the pH-Time Cell Arrangement . . . . .	21
5.	Schematic Diagram of the pH-Time Testing Apparatus . . . .	22
6.	Typical Potential-Load Curves . . . . .	26
7.	Schematic Diagram of the Final Portion of the Potential- Load Curves . . . . .	28
8.	General Shape of the pH-Time Curve . . . . .	30
9.	pH-Time Curves for the Materials Tested, Showing Differences in "Incubation" Times . . . . .	33
10.	Potential-pH Curves for Pure Titanium, Showing the Effect of pH on Potential . . . . .	36
11.	Standard Potential-pH Diagram for Titanium. The Dotted Path AB Shows the Variation of Potential with pH (See Figure 10) . . . . .	39



## SUMMARY

This research was undertaken to study the electrochemical conditions and changes occurring at the tip of a propagating stress corrosion crack in titanium and some titanium-aluminum alloys. In the first part of the study electrochemical measurements were made on tensile specimens to record the variations of the potential with load, up to fracture. The results confirm the importance of the condition of the passive film on the metal surface in the SCC process.

The main study concerned the simulation of the conditions at the crack tip by scratching a specimen with a diamond tool in a special cell with separate anodic and cathodic compartments. The pH and potential changes were measured and recorded. The results show that an initial "incubation" time, with no pH change, occurs at the beginning of the experiments. Then the pH starts to decrease until a steady state is reached. The absence of oxygen is a necessary condition for the pH drop.

The data seems to indicate that the direct formation of  $TiO_2$  takes place, without the formation of intermediate oxides. According to the potential and pH data, the results agree with the conditions established by the Pourbaix diagram for titanium.



## CHAPTER I

### INTRODUCTION

The purpose of this study is an investigation of the electrochemical conditions at the tip of a stress corrosion crack. The knowledge of such conditions is essential in understanding the process, since it is at the crack tip where the most significant events occur during the cracking.

Before entering a detailed discussion of this research, it is in order to first review the characteristics and the mechanisms of stress corrosion cracking in titanium alloys.

#### Stress Corrosion Cracking Characteristics

Stress Corrosion Cracking (SCC) is a general term to indicate a form of cracking deriving from the combined effects of stress and exposure to a specific environment. Some general features are common to the materials susceptible to SCC:

- (1) The susceptibility to SCC is primarily restricted to alloys, while pure metals are generally immune;
- (2) The environment causing SCC is relatively specific for each alloy system;
- (3) The presence of an effective tensile component of the stress is required; and
- (4) The cracking mode can be either intergranular, transgranular, or a mixture of both.



The gravity of the problem of SCC in industry is due to the following characteristics of the phenomenon:<sup>1</sup>

(a) Materials generally passive or with a low corrosion rate in a specific medium may be subject to catastrophic failure by SCC when exposed to stress.

(b) The stress required for cracking under SCC conditions is only a fraction of the stress needed for failure in an inert environment.

(c) A small amount of the attacking species is sufficient to cause SCC in an otherwise inert medium. For example, impurities in environments generally believed completely non-aggressive, such as air or distilled water, can be sufficient to cause cracking.

(d) Stress corrosion cracks can propagate through a material without externally applied stress if residual tensile stresses, resulting from casting, machining or welding, exist.

Among the materials showing susceptibility to SCC, titanium and its alloys have been shown to crack in a greater variety of environments than most alloys. The commercial use of titanium started in 1952, when the defense industry became interested in its high temperature strength and low density compared to steel. Although titanium itself is a very reactive metal, it is covered by a tenacious passive film and its alloys were initially believed to be immune in the environments commonly causing SCC.

In 1953 the first report on SCC of titanium in fuming nitric acid was issued<sup>2</sup> and in 1965 titanium alloys were found susceptible in aqueous environments at room temperature.<sup>3</sup> Now titanium and its alloys are known to crack in such a variety of environments as methanol, seawater, dinitrogen tetroxide, mercury and solid cadmium.



### Parameters Influencing SCC of Titanium Alloys

The SCC of titanium alloys in aqueous environments is influenced by three external parameters: metallurgical, mechanical and environmental.<sup>4</sup>

#### Metallurgical Parameters

Pure titanium exists in a hexagonal close-packed structure, called  $\alpha$ , at room temperature. It undergoes a transition to a body-centered cubic phase,  $\beta$ , at 1625°F. When titanium is alloyed to other elements the stability of one phase is usually enhanced with respect to the other; aluminum, for instance, is a stabilizer of the  $\alpha$  phase, raising the temperature of the  $\beta$  transformation. Experimental evidence has shown that the factors promoting SCC are structure dependent, and studies have been made to detect the specific causes.

Most commercial  $\alpha$ -phase alloys contain one or more of these elements: O, Al, Sn and Zr. Pure titanium containing approximately 1200 ppm of oxygen is immune to SCC. Increasing the oxygen content, or adding Al, promotes SCC susceptibility. The critical Al content is about 5%, above which SCC occurs in binary alloys in aqueous solutions. At higher Al contents the phase  $Ti_3Al$  can precipitate during low temperature ageing, further decreasing the SCC resistance. A similar effect is produced by the addition of Sn, which generally decreases the resistance to SCC, while apparently an increase in Zr content reduces the susceptibility in aqueous solutions.

Williams<sup>5</sup> studied the fractography of several ( $\alpha + \beta$ ), two-phase alloys containing different amounts of aluminum. An examination of the fracture surface showed a slow crack growth region followed by a region



of fast fracture. Williams concluded that in the slow cracking region the  $\alpha$  phase acts as the susceptible element, causing transcrystalline cleavage, while the  $\beta$  phase acts as a crack arrestor, failing by ductile fracture.

The observed increase in susceptibility for alloys containing more than 5% Al was explained by a change in the dislocation structure. At above 5% Al in binary alloys the dislocations exist in coplanar arrays; in association with these arrays large local stresses are generated, that increase the SCC susceptibility of the  $\alpha$  phase, due to restricted slip in only a few slip systems. On the other hand, SCC resistance improves with the addition of elements like Mo or V, that act as stabilizers of the  $\beta$  phase, that is a crack arrestor.

As far as  $\beta$ -phase alloys are concerned, studies have shown that more than 10% Mn causes susceptibility in the  $\beta$  phase; in general, it can be said that additions of Cr and Mn promote susceptibility, that decreases with additions of Mo and V.

One effective way to improve SCC resistance in titanium alloys is through composition control; other available means are heat treatment, to change the composition of the  $\alpha$  and  $\beta$  phases, grain size, dislocation structure, order, etc.

#### Mechanical Parameters

Titanium alloys can be compared according to the requirement of a stress concentrator to produce SCC. Most  $\beta$ -phase alloys, together with a few  $\alpha$ -phase and ( $\alpha + \beta$ ) alloys, are susceptible only in the presence of a sharp notch, while this is often not necessary for other alloys.

The thickness of the specimen can also be important; this is true



for some  $\alpha$  and  $(\alpha + \beta)$  alloys, where the SCC susceptibility decreases with decreasing thickness. This has been attributed to a change from plane strain to plane stress fracture toughness conditions.

The rate of loading can also be a factor influencing the susceptibility in some alloys; Powell and Scully<sup>6</sup> observed that the SCC of  $\alpha$ -phase alloys in seawater occurred over a relatively narrow range of loading rates, and ductile fracture occurred outside these limits.

An important aspect in neutral aqueous solutions is the existence of a threshold value of stress intensity ( $K_{ISCC}$ ) below which SCC is not believed to occur. However, the absence of cracking after a relatively long time does not exclude in itself the possibility of a cracking velocity too low to be detected in the tests performed.

#### Environmental Parameters

The halide ions  $Cl^-$ ,  $Br^-$  and  $I^-$  are capable of influencing the SCC susceptibility of titanium alloys either by promoting cracking in an otherwise immune environment or by increasing the speed of cracking with increasing halide concentration.

The SCC velocity is strongly influenced also by the potential. Beck<sup>7</sup> derived an equation predicting a linear relationship between velocity of cracking and potential; similar linear relations have been shown in cases involving a number of titanium alloys.

Changes in crack velocity have been observed with variations in temperature and viscosity of the environment. The cracking velocity generally increases with temperature, but this relationship holds only in some instances, while in other cases the temperature seems to have little effect. Finally, it has been reported that an increase in viscosity of the environment generally produces a decrease in crack velocity.



### Stress Corrosion Cracking Theories

The mechanisms proposed for the SCC of titanium alloys can be divided in the following groups:

Brittle Oxide Rupture. Discontinuous formation and fracture of a brittle oxide film at the crack tip, with the film repair at the surface considered the rate controlling process.

Stress Sorption. Lowering of the surface energy due to the adsorption of ions at the crack tip.

Hydrogen Embrittlement. Diffusion of hydrogen into the metal causing embrittlement of the lattice or the formation of brittle hydrides.

Mechano-Chemical. Preferential anodic dissolution at the crack tip at particularly active sites sensitized by strain and the disarray of the metal.

Mass Transport-Kinetic. Electrochemical and kinetic data are used to formulate a quantitative model for the events occurring at various regions inside a crack.

### Brittle Oxide Rupture Theory

The theory was first introduced by Logan,<sup>8</sup> and McEvily and Bond<sup>9</sup> used it to explain fracture of  $\alpha$ -brass in "tarnishing" ammonia environments. The essential features of this model are the following:

- (1) Exposure of the metal to the environment rapidly produces a protective film, reducing the corrosion rate to a low level;
- (2) As the film increases in thickness its resistance to fracture lowers, due to its brittleness and the probable presence of epitaxial stresses. At a certain point the film breaks and the resulting crack



advances to the oxide-metal interface, where it is arrested by plastic blunting;

(3) Another layer of film grows on the surface of the bare metal exposed to the environment by the crack, and, when a critical thickness is again reached, the process repeats itself through a series of discontinuous steps.

A characteristic feature of this type of cracking is the presence of striations on the fracture surface. These are believed to indicate progressive positions of crack arrest and growth. A similar film breakdown mechanism is now believed to occur for several titanium alloys in oxygenated dinitrogen tetroxide.<sup>10</sup>

Another model<sup>11</sup> involves the behavior of a surface film as the main process responsible for the initiation and propagation of SCC. According to the authors the following events take place:

(1) When physical rupture of the protective film occurs, fresh metal surface is exposed to the environment;

(2) While the passive film starts to reform, certain specific ions, such as  $\text{Cl}^-$ ,  $\text{Br}^-$ , and  $\text{I}^-$ , migrate to the exposed metal surface, hindering the repair of the film;

(3) The delay in repassivation causes the formation of a corrosion tunnel, due to the formation and hydrolysis of metal halides.

The ability of an oxide film to repair itself is a major factor influencing the cracking rate; to accelerate the reformation of the film cathodic polarization can be used, as well as the addition of ions that favor repassivation in a specific environment. An alternate way is through metallurgical treatments to prevent film rupture: heat treatment,



selection of alloying elements and improved design can help achieve the best film resistance.

### Stress Sorption Theory

This mechanism, first suggested by Petch and Stables<sup>12</sup> to explain hydrogen embrittlement in steels, postulated the adsorption of hydrogen on dislocation-formed crack nuclei, causing their stabilization and propagation at lower stress levels. The stabilization results from the reduction in surface energy of the metal, associated with hydrogen adsorption. Uhlig<sup>13</sup>, and Coleman and others<sup>14</sup> proposed a similar process for SCC in metals and alloys. The weakening of surface energy is believed in these cases due to the adsorption of some chemical species capable of reducing the attractive forces between the atoms at the tip of the crack, where plastic deformation already plays a role in weakening the bonds.

The stress sorption mechanism can explain some characteristics of SCC, i.e.:

- (1) Since chemisorption is a very specific process, this can account for the selectivity in SCC between metal and environment;
- (2) The beneficial effect of cathodic protection is explained by the shift in potential into regions where the damaging ions cannot be adsorbed. A shift towards more negative potentials (cathodic polarization) makes reasonable the assumption that adsorption of ions be inhibited. The effect of extraneous anions can be explained this way, or by the fact that, in sufficient concentration, they would tend to displace species already adsorbed;
- (3) The brittle SCC failures observed in glass and plastics in specific environments can be explained analogously to metals.



This theory, however, cannot explain the immunity of pure metals to SCC. The possibility has been advanced<sup>15</sup> that chemisorption occurs not on the entire surface, but at particular active sites in the metal, such as emerging dislocations. Adsorption is a process that requires a certain amount of time, so the active site must remain at the metal surface for a sufficient period. In this respect the presence of solute atoms, second-phase particles, interstitial and impurity atoms, etc., can impede the movement of imperfections and extend their surface life long enough for chemisorption to occur. In pure metals the dislocations could escape the surface in less time, so that the adsorption might be negligible.

It has been suggested<sup>14</sup> that electrochemical processes may be responsible for the removal of oxide films initially present at the metal surface, and also for the prevention of fast repair of oxide films mechanically ruptured by stress. Electrochemistry may also play a role in the formation of metal complexes that, in some metal-environment systems, are believed to be the adsorbing species in place of single ions.

#### Hydrogen Embrittlement Theory

Evans<sup>16</sup> and Edeleanu<sup>17</sup> first suggested that the pickup of hydrogen at the crack tip embrittles a metal lattice enough to allow further crack propagation. The hydrogen is supposed to be derived by local reduction of hydrogen ions produced at the crack tip and excess ions in the solution as the result of the formation of oxide films or hydroxides. The hydrogen discharged at cathodic areas may not play as an important role in the process, since diffusion is limited by dimensions in the crack and by the presence of oxide on the metal surface.



In titanium alloys two types of hydrogen embrittlement can occur:<sup>18</sup>

High Strain-Rate Embrittlement. Due to thermal precipitation of hydrides. It is mostly evident in  $\alpha$ -phase alloys and becomes more pronounced with low temperature, higher strain rates, increased hydrogen content and with a notch present;

Low Strain-Rate Embrittlement. Occurs at hydrogen contents lower than necessary for hydride precipitation. It is mainly present in  $\alpha$  and ( $\alpha + \beta$ )-phase alloys and increases in effect with increasing hydrogen content, lower strain rate, and at temperatures near room temperature.

The effect of the above variables is explained by considering hydrogen diffusion into the metal at preferred sites as the cause of embrittlement. Gray<sup>19</sup> has proved the presence of a high hydrogen concentration near the fracture surface in the hot salt cracking of Ti-8Al-1Mo-1V, and concluded that the embrittlement was caused by hydrogen diffusion and segregation to regions of high stress concentration.

The mechanism of hydrogen embrittlement for Ti alloys in aqueous environments has been extensively studied in recent years by Scully and his co-workers. The crack initiation and propagation processes have been discussed in detail.<sup>6</sup> The initial step is the breakdown of the passive film on the surface by the stress, and a critical factor is represented by a delay in repassivation, enabling hydrogen to enter the metal lattice. The reasons for the delay are not well known, but they include the preferential adsorption of species other than hydrogen on the fresh metal surface and the nature of the deformation processes at the crack tip.

The transgranular cleavage occurring as a result of hydrogen entry has been explained<sup>20</sup> as a form of slow strain-rate hydrogen embrittlement.



The adsorption of hydrogen with hydride formation is preferred over the idea of chloride ion adsorption, since the diffusion rate of this ion into titanium would be much lower than for hydrogen.

The formation of hydrides restricts lattice ductility, since it can occur on two of the three slip systems of the titanium lattice, providing a barrier to dislocation movement.

As mentioned before, SCC was observed over a narrow range of crosshead speeds;<sup>6</sup> to explain ductile fracture at high crosshead speeds it was postulated that no time was allowed for sufficient hydrogen adsorption, while at low crosshead speeds no cracking occurred since the passive film had sufficient time to repair itself.

Since the speed of hydrogen diffusion is much lower than the average crack velocity, Scully<sup>21</sup> mentioned several possibilities to explain this seeming contradiction. It is possible that the hydrogen diffusion is higher than calculated when the lattice is deforming, or that hydrogen may only initiate cleavage, which can propagate without further assistance from the embrittling species.

To explain the occurrence of SCC in hydrogen-free environment, as  $\text{CCl}_4$ , Scully postulated that this is due to moisture in the gas, causing hydrolysis reactions with production of chloride ions.

#### Mechano-Chemical Theory

A mechanism where electrochemistry and mechanical stress play related roles in the cracking was developed by Hoar and Hines.<sup>22</sup> Starting from the consideration that stresses and an electrochemical anodic reaction have an essential part in the cracking, since load removal and cathodic polarization both stop the process, a joint mechanical-



electrochemical mechanism was presented. The propagation of cracks is supposedly due to anodic dissolution assisted by strain and lattice disarray, without appreciable polarization occurring at the base of the crack. The regions of lattice disarray can be grain or subgrain boundaries, emergent dislocations, zones of strain caused by cold work, etc. The presence of such imperfections on a metal surface has long been considered responsible for the higher electrochemical reactivity of cold worked and fine grained materials compared to annealed metals and single crystals.

Hoar<sup>23</sup> proposed that the increase in dissolution rate is not due in itself to the increase in active sites as the result of the initial plastic deformation, but rather to the presence of local stresses that continuously feed active sites to the metal surface. This could explain how plastic deformation just ahead of a stress corrosion crack could promote rapid dissolution of the surface atoms at the crack tip, while the crack walls dissolve at a very low rate.

The mechano-electrochemical mechanism can explain the observation that materials showing coplanar dislocation arrays are more susceptible to SCC, since such dislocation structure favors restricted slip during yielding and this can result in a great increase in anodically active sites. Under these conditions the propagation of a crack under electrochemical dissolution might be possible.

#### Mass Transport-Kinetic Theory

Beck<sup>24</sup> has developed a quantitative theory for the electrochemical kinetic and mass transport processes inside a propagating stress corrosion crack on the basis of the following fundamental assumptions:



(1) The crack velocity is low compared to the velocity for electrochemical processes to occur inside the crack, so that a steady state is reached;

(2) The crack walls are considered straight and the crack angle small, about  $4^\circ$ . The crack tip is blunted at a certain distance from the apex;

(3) The electrolyte completely fills the crack;

(4) The kinetic and electrochemical reactions for plane electrodes are applied to events occurring inside the crack.

This model, called mass transport-kinetic (MTK) model, considers three basic regions inside a crack: the tip zone, where cleavage occurs, a "monolayer" zone, where a first monolayer of oxide has been formed on the crack walls, and a "multilayer" zone, where the oxide increases in thickness. The formation of titanium halide at the crack tip is believed to be the reaction responsible for SCC. The halide rapidly hydrolyzes and the hydrogen formed enters the metal lattice.<sup>25</sup>

In the "monolayer" zone oxidation of the metal occurs, accompanied by hydrogen ions reduction and displacement of halide ions from the titanium halide present or adsorbed in this region. Analogous titanium oxidation occurs in the "multilayer" zone.

The MTK model has been formulated in agreement with electrochemical and kinetic principles, but it suffers from limitations. The principles used are not strictly valid at the crack tip, because of the atomic-scale mechanisms involved, and the reactions occurring there are not considered. Furthermore, the exact crack tip angle is not known, and this hampers the precision of Beck's calculations, as does the limited accuracy of the



kinetic data used. Finally, the formation of soluble titanium ions has not been taken into consideration, due to lack of kinetic data, while the Pourbaix diagram indicates that soluble species are thermodynamically stable for the conditions present at the crack tip.

Controversy still exists about which one of the mentioned theories applies to the SCC of titanium alloys in seawater; the purpose of this research is to contribute to the understanding of the electrochemistry of the process. In the first part of the study variations of the electrochemical potential with load will be studied on tensile specimens at increasing loads up to fracture. The main purpose of this research will, however, concern the simulation of the conditions existing at the tip of a stress corrosion crack.

#### The Occluded Cell Corrosion

In a SCC process the geometry of the crack plays a major role in establishing the environmental factors that affect the cracking. A propagating SCC crack is generally very long compared to its width; the results are:

- (1) A very limited amount of solution is present inside the crack;
- (2) The diffusion of ions from the bulk solution to the crack tip is greatly reduced;

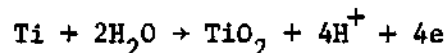
- (3) A very low oxygen concentration is present at the crack tip.

As a consequence of all these factors there can be a drastic difference in chemical nature between the solution at the crack tip and the bulk solution.

Recently Brown<sup>26</sup> has proposed the term "occluded cell corrosion"



in every case of localized corrosion where an acid condition is present at the site of attack. The acidity is the result of hydrolysis of metal ions and is maintained by the restricted interchange of solution. In the case of SCC of titanium, the hydrolysis reaction is the following:



and, as a result, the pH is expected to decrease inside the crack.

Local acidification by hydrolysis was first acknowledged by Hoar in 1937<sup>27</sup> and Edeleanu in 1959<sup>28</sup> postulated acidity in stress corrosion cracks, due to the same reason. Brown<sup>29</sup> succeeded in measuring the pH of a stress corrosion crack tip by using a freezing technique; more recently,<sup>30</sup> by using a combination of glass and antimony electrodes, he was able to measure the pH of the crack tip in situ.

In trying to reproduce experimentally the conditions at the crack tip, an apparatus was used in this research that can be considered a modification of the setup used by Beck, et al.<sup>31</sup> The basic principle in common is the exposure of fresh metal surface to the environment by scratching the specimen with an appropriate tool.



## CHAPTER II

### EXPERIMENTAL PROCEDURE

#### Potential-Load Experiments

To measure the variation of electrochemical potential with load, tensile specimens were prepared using rolled sheets of Ti-5Al and Ti-7.5Al alloys, whose composition is shown in Table 1.

The environment used to produce SCC was a 3.5% solution of NaCl, contained in a plastic cup sealed around the specimen. The specimens were first polished with 400 grit emery paper, then coated with silicone rubber, leaving only a small "window,"  $1 \text{ cm}^2$  in area, unprotected.

The testing apparatus, shown in Figure 1, consisted of an ARA pneumatic testing machine; the specimens were generally preloaded at a value under  $K_{ISCC}$ , to shorten the length of the test, then loaded 20 lbs. at a time, at 40 seconds intervals, to fracture. A standard calomel electrode, placed near the uncoated surface of the specimen, was used to measure the specimen potential and a recorder provided the potential versus load curve. A detail of the cell arrangement is shown in Figure 2.

#### pH-Time Experiments

The apparatus used in these tests is illustrated in Figures 3, 4 and 5. It was composed of a small plastic cell connected to a large beaker through a glass tube. A fritted glass membrane separated the two compartments, while allowing an electrical connection.

The scratching system was composed of a small diamond-tipped tool,



Table 1. Analysis of the Titanium and Titanium-Aluminum Alloys Tested

<u>Material</u>	<u>Composition in Percent</u>					
	<u>Al</u>	<u>Fe</u>	<u>N</u>	<u>O</u>	<u>C</u>	<u>H</u>
Pure Ti	-	0.028	0.002	0.075	0.024	0.004
Ti-2Al	2.09	0.026	0.002	0.065	0.026	0.003
Ti-5Al	5.10	0.034	0.002	0.052	0.026	0.005
Ti-7.5Al	7.76	0.014	0.002	0.062	0.024	0.006



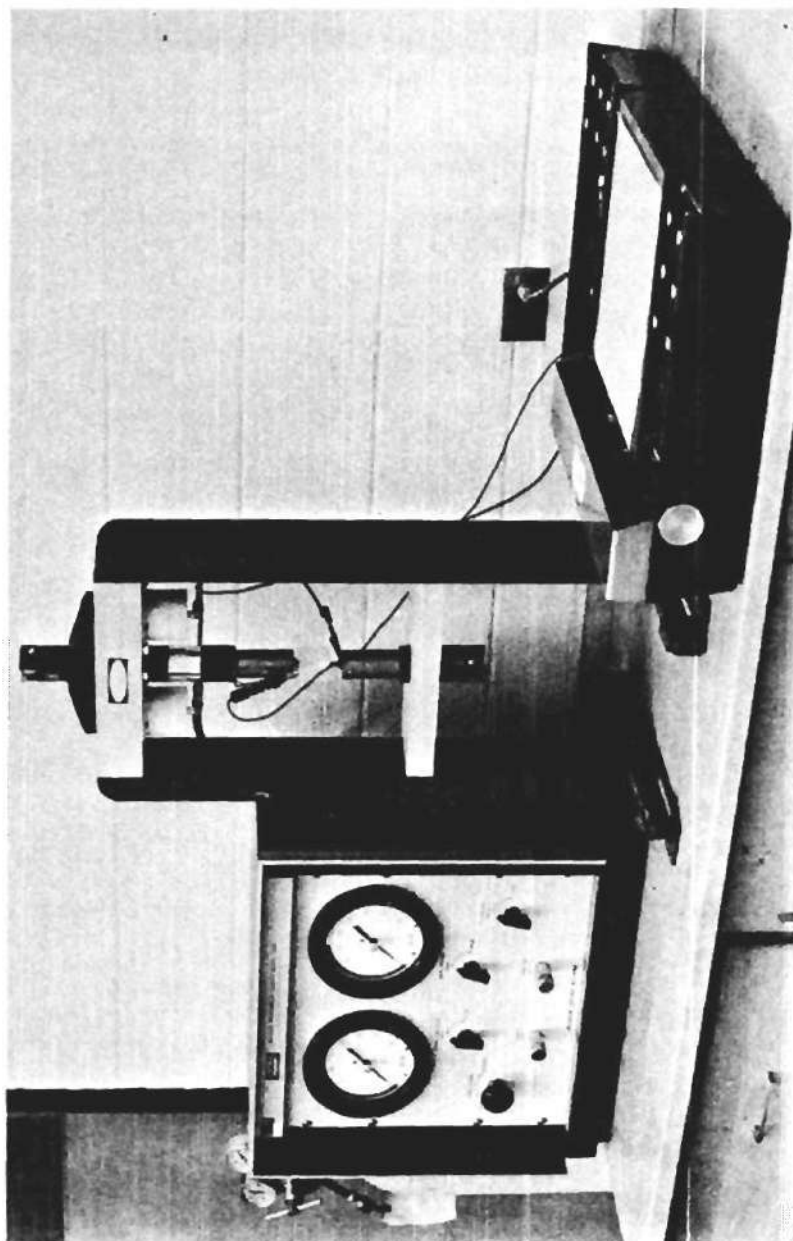


Figure 1. General View of the Potential-Load Testing Apparatus



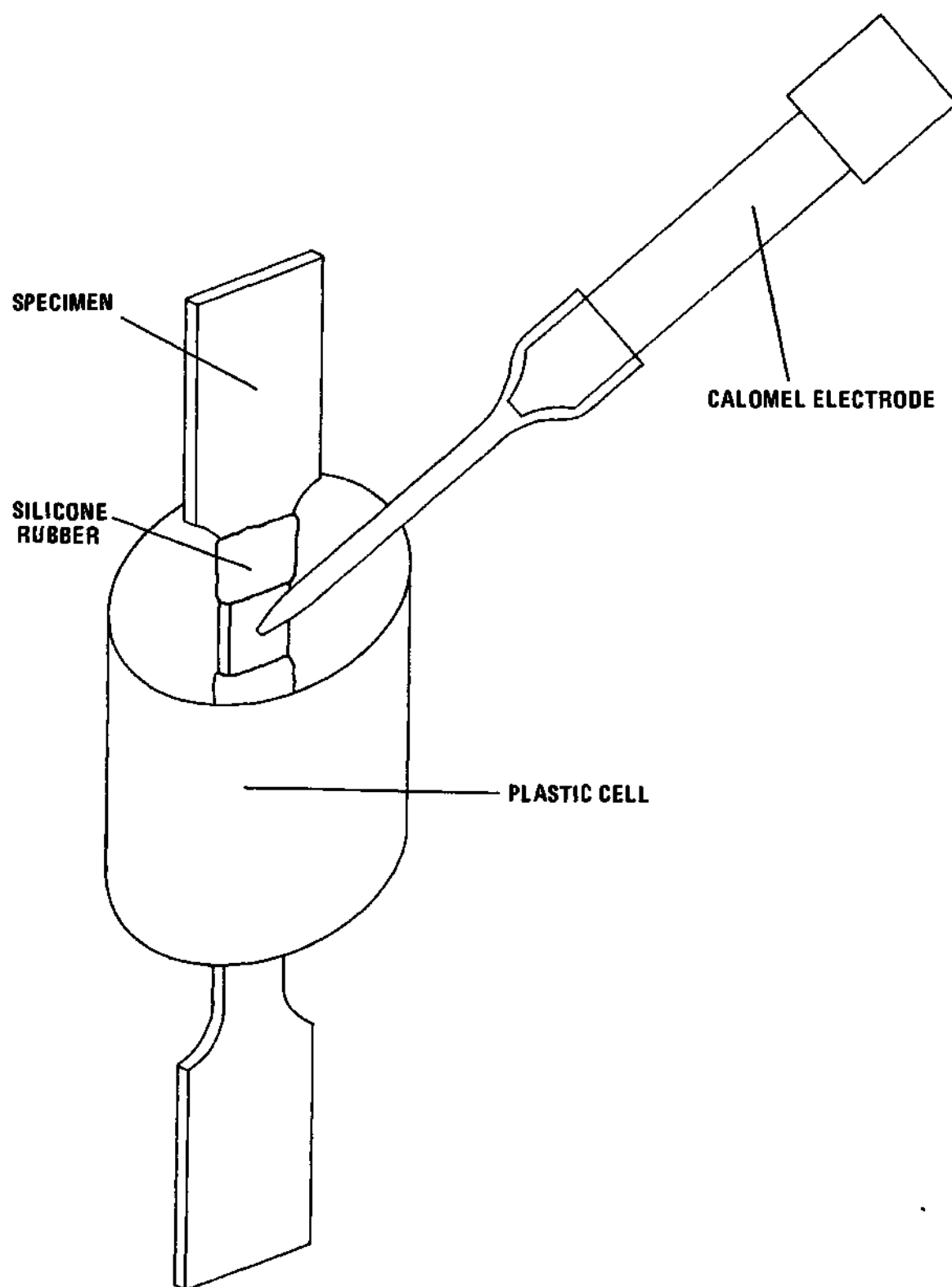


Figure 2. Detail of the Potential-Load Cell



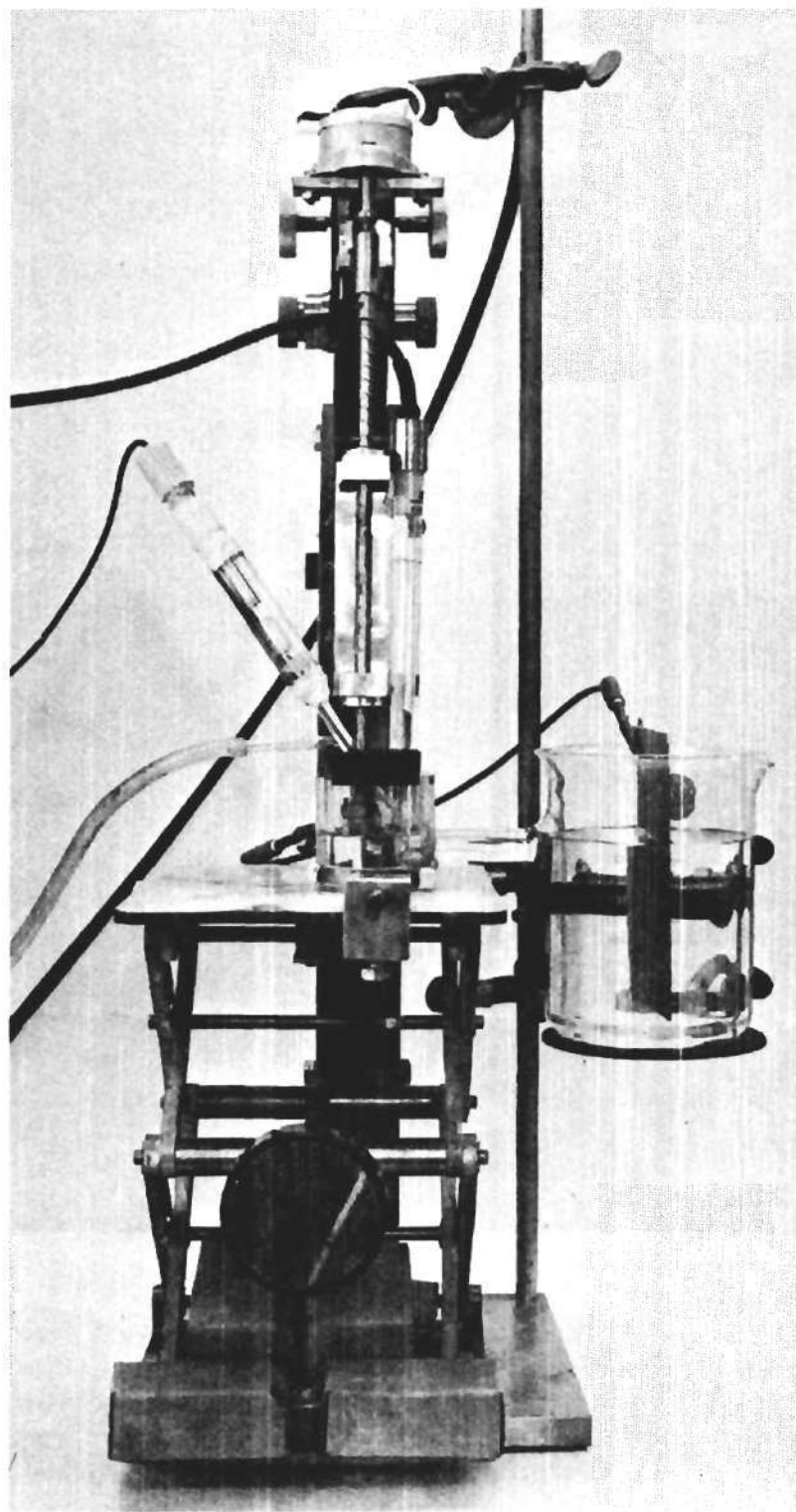


Figure 3. General View of the pH-Time Testing Apparatus



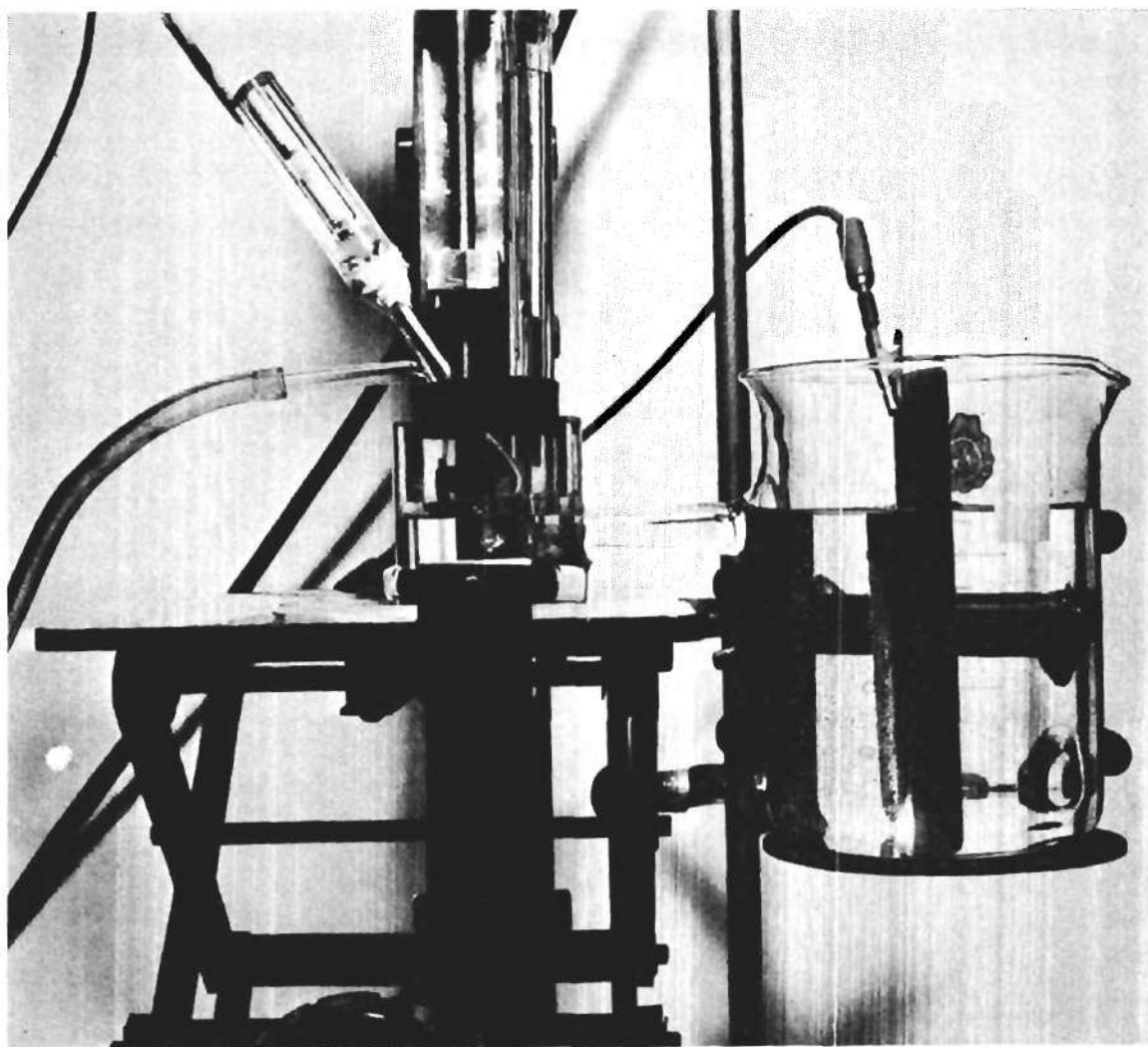


Figure 4. Details of the pH-Time Cell Arrangement



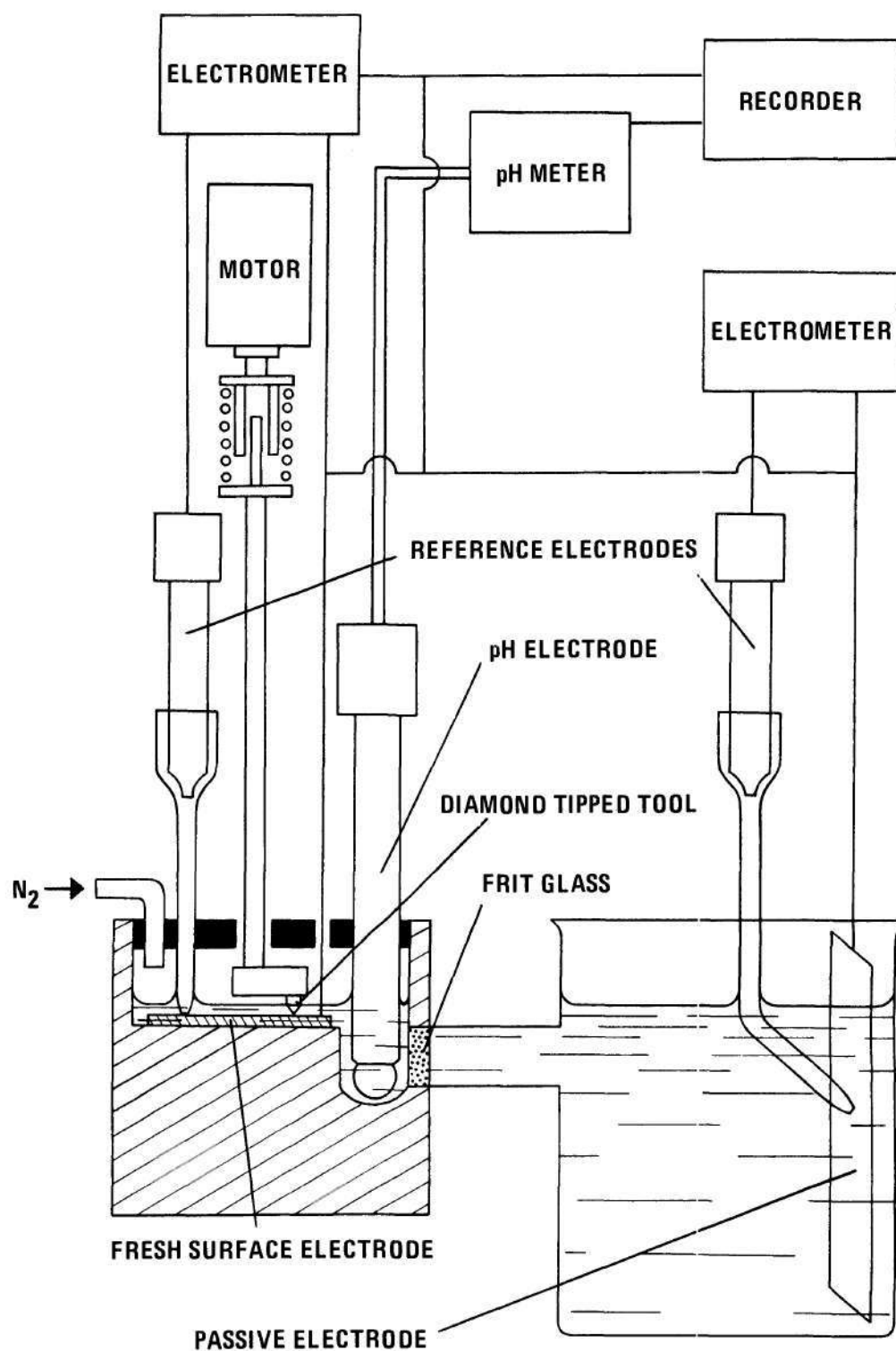


Figure 5. Schematic Diagram of the pH-Time Testing Apparatus



driven eccentrically in a small circle at 8 rpm by a synchronous motor. The tool was coated with silicone rubber to avoid corrosion of the tool itself and only the diamond tip was left uncoated. The whole motor-tool system could be raised and lowered by means of micrometric knobs, to apply the proper pressure to the tool on the specimen. For the same purpose a spring between the motor and the tool shaft kept a uniform pressure on the tool during the rotation.

The scratching exposed fresh metal to the environment, simulating the tip of an advancing stress corrosion crack; an outside counter-electrode simulated the passive area outside the crack.

The materials studied consisted of pure titanium and three titanium-aluminum alloys, whose compositions are given in Table 1. The specimens were disc-shaped, polished with 400 grit emery paper and then coated with a thin layer of paraffin. The purpose of the coating was to avoid the presence of a large area of passive metal which would act as a cathodic site inside the test compartment. The specimen was fixed to the bottom of the test cell by means of two plastic screws, and a large electrode of the same test material was placed inside the beaker.

The environment used was a 3.5% NaCl solution; a small quantity of it, for most experiments 2.7 cc, was first deaerated with nitrogen and then placed in the test cell. The purpose of the deaeration was to simulate the condition of low oxygen concentration inside a crack. To insure deaeration during the experiment, the test cell was kept sealed and nitrogen was constantly pumped inside of it. The large beaker was filled with the same 3.5% NaCl solution, but not deaerated, maintained at the same level as in the small cell. The purpose of the fritted glass membrane



between the two cells was to simulate the high resistance path, electrical and/or chemical, between the solution at the crack tip and the bulk of the corroding environment.

The pH measurements were carried out in the small cell using a combination glass-reference electrode. Two auxiliary saturated calomel electrodes measured the potential of the single electrodes. A Sargent-Welch model NX pH meter was used to monitor visually the pH and a recorder was used to obtain the pH versus time curves.

The solution in the test compartment was analyzed, during and at the end of the experiments, to detect the presence of titanium ions using a hydrogen peroxide indicator. For the titanium-aluminum alloys the solution was also analyzed for the presence of aluminum ions, using aluminon as the indicator.



### CHAPTER III

#### DISCUSSION OF RESULTS

##### Potential-Load Curves

Typical potential versus load curves are shown in Figure 6. The potential values given in the ordinate are only indicative of the shifts from the initial value to positive and negative directions and are not absolute values. All the materials tested showed the same behavior. Curve (a) represents the results when testing immediately after exposure to the environment, while curve (b) is for materials tested after exposure to the solution for a period of 24 hours.

Initially curve (a) shows a period where the potential remained constant, except for small variations to positive values every time a load increase was applied. With increasing load a point was reached when the potential started to shift to negative values, and at the same time the small variations with increasing load disappeared. In the final portion of the curve the potential shifted again to positive values; the potential variations then became increasingly larger up to the fracture of the specimen which coincided with a very large jump in the potential.

For specimens left for 24 hours in the solution, curve (b), the behavior is essentially the same, with the exception that no shift of the potential to negative values was observed, instead the potential gradually changed to more positive values continuously through the experiment.

Several specimens were left in the solution for different periods of time before testing. The effect of this exposure on the final portion



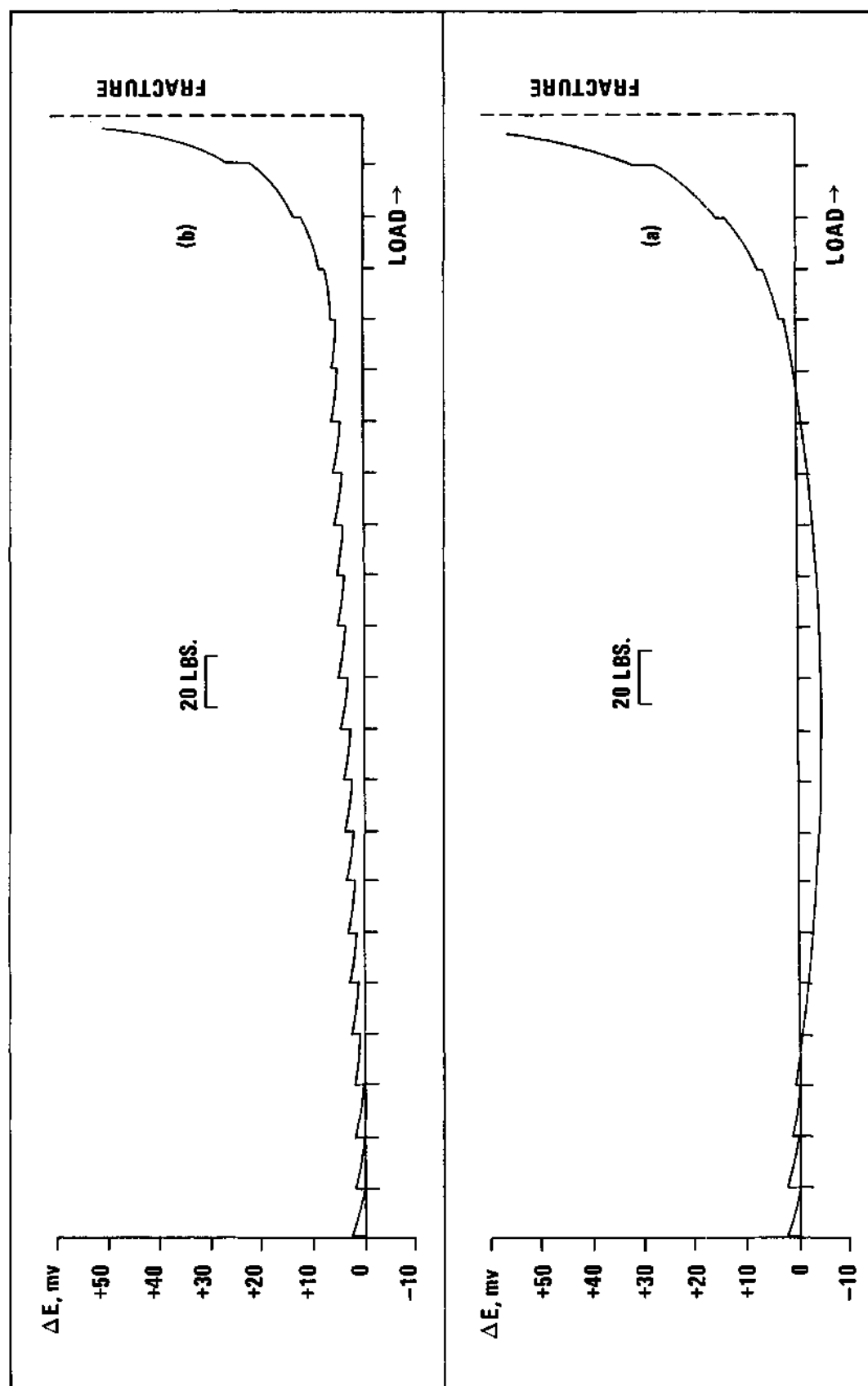


Figure 6. Typical Potential-Load Curves



of the potential versus load curves is shown schematically in Figure 7. The slope of the experimental curves increases with the increase of time of exposure to the environment.

In examining the curves of Figure 6, the following conclusions can be drawn. At the beginning of the experiments the small potential shifts to positive values at the onset of each increase in load can be attributed to the breakdown of the surface passive film causing the metal to become active in that area. The reformation of the film is seen by the gradual return of the potential to its initial value between two successive loadings. The behavior of the specimen represented by curve (a) in Figure 6, i.e., disappearance of the small potential jumps and shift of potential to negative values with increased loading, is not readily explained. The most probable hypothesis concerns the relaxation of residual stresses due to cold working once certain stress levels have been reached. This process seems to proceed continuously over a given load range until all the stresses have been relieved in the area concerned. In the final part of the curve film restoration is again achieved until at very high stress levels the deformation of the material exceeds the speed of film repair. Hence more fresh metal is exposed and the potential becomes more and more positive until fracture occurs.

The different behavior shown in curve (b) could be explained by the growth of the passive film due to prolonged exposure to the environment. This may screen out the effect of the stress relaxation. The same hypothesis could be advanced as an explanation of the behavior shown in Figure 7. The difference in slope with different exposure times could be related to the formation of films of greater thickness with increasing time.



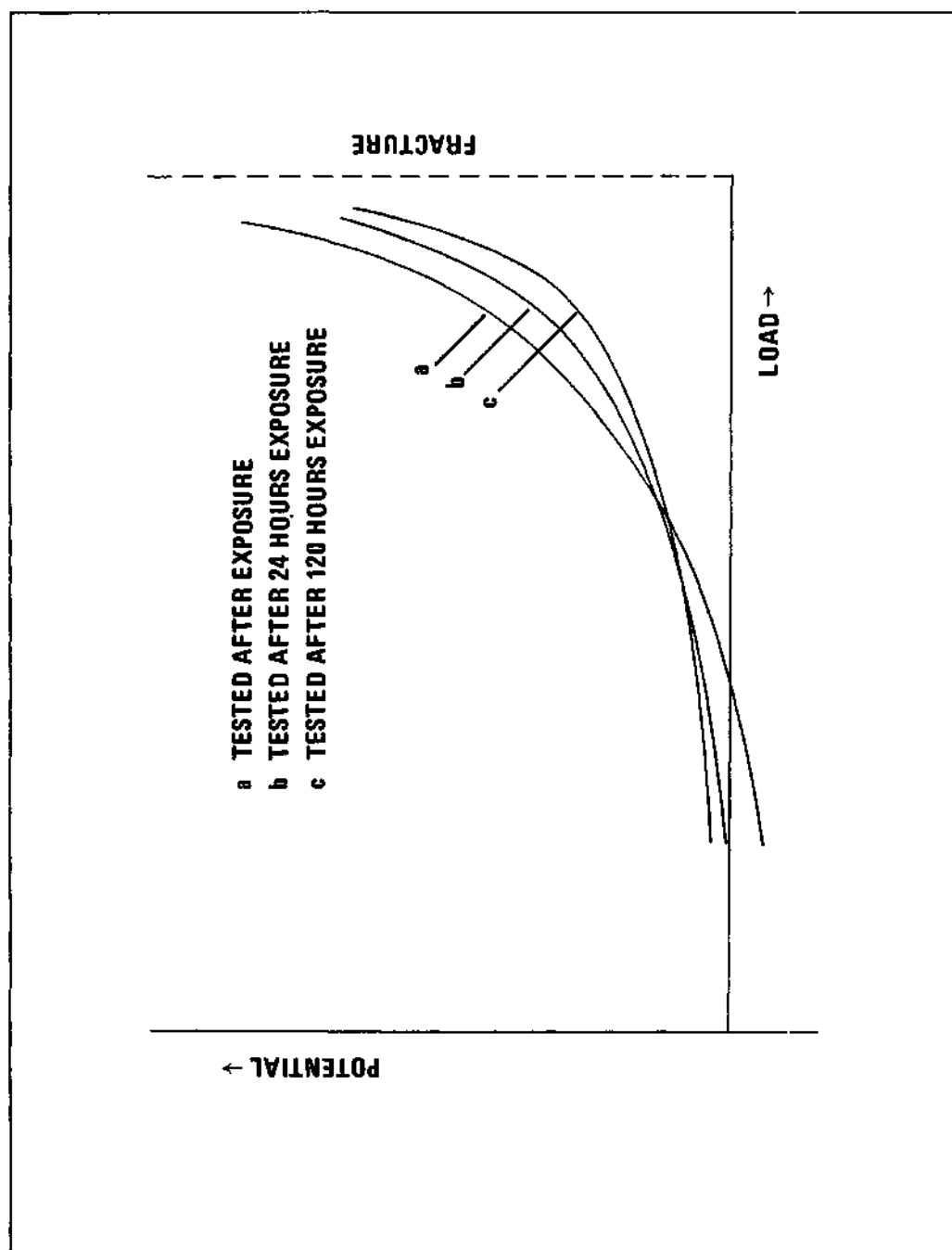


Figure 7. Schematic Diagram of the Final Portion of the Potential-Load Curves



### pH-Time Curves

A typical pH-time curve is shown in Figure 8. Several distinct features can be observed: after the start of each experiment an "incubation" time was noticed where generally no pH change was observed. In some occasions the pH actually increased during this period. After the "incubation" period the pH started to decrease; in the final portion of the curve the slope decreased steadily, until ultimately the pH became relatively constant and independent of time.

The final stage was reached in a period of 4 to 5 hours, after which the experiment was stopped. However, some experiments were continued to observe the absolute minimum pH values that could be reached for each of the materials tested. These experiments lasted 24 to 48 hours, i.e., until the pH had reached an apparently stable value.

Table 2 gives the lowest pH value recorded for each of the materials tested. All of the curves obtained showed the above mentioned features; however, the rate of the pH decrease underwent some slight variations when testing two different materials and also when testing twice the same specimen. The largest variations were observed in the "incubation" times which were reasonably constant for every material but differed greatly for different materials; this can be noted from Table 3. A set of curves for the different alloys is represented in Figure 9, showing the differences in "incubation" times, slope, etc.

In discussing a typical pH-time curve, the initial "incubation" time could be explained by the presence of residual oxygen in the solution. In this case, the hydrogen ions produced by hydrolysis can react with the oxygen with formation of water resulting in no pH change. The pH increase



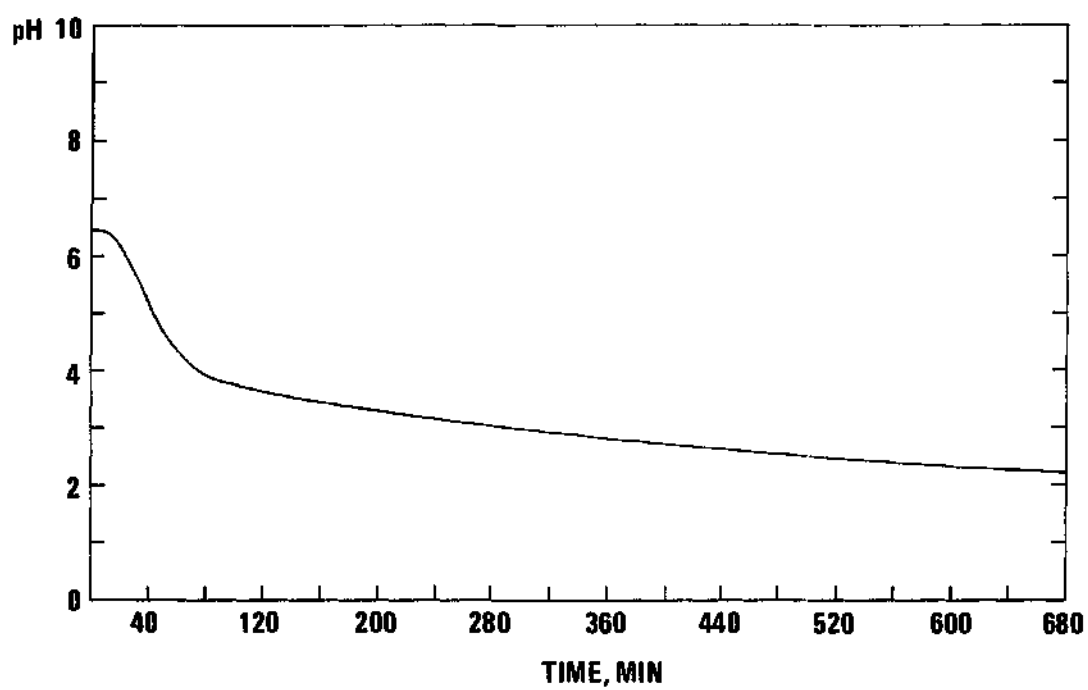


Figure 8. General Shape of the pH-Time Curve



Table 2. Lowest pH Values Recorded for the Materials Tested.

Material	pH
Pure Ti	1.89
Ti-2Al	1.96
Ti-5Al	2.09
Ti-7.5Al	1.90



Table 3. "Incubation" Times for the Materials Tested.

Material	Incubation Period
Pure Ti	42 min.
Ti-2Al	14 min.
Ti-5Al	9.5 min.
Ti-7.5Al	8 min.



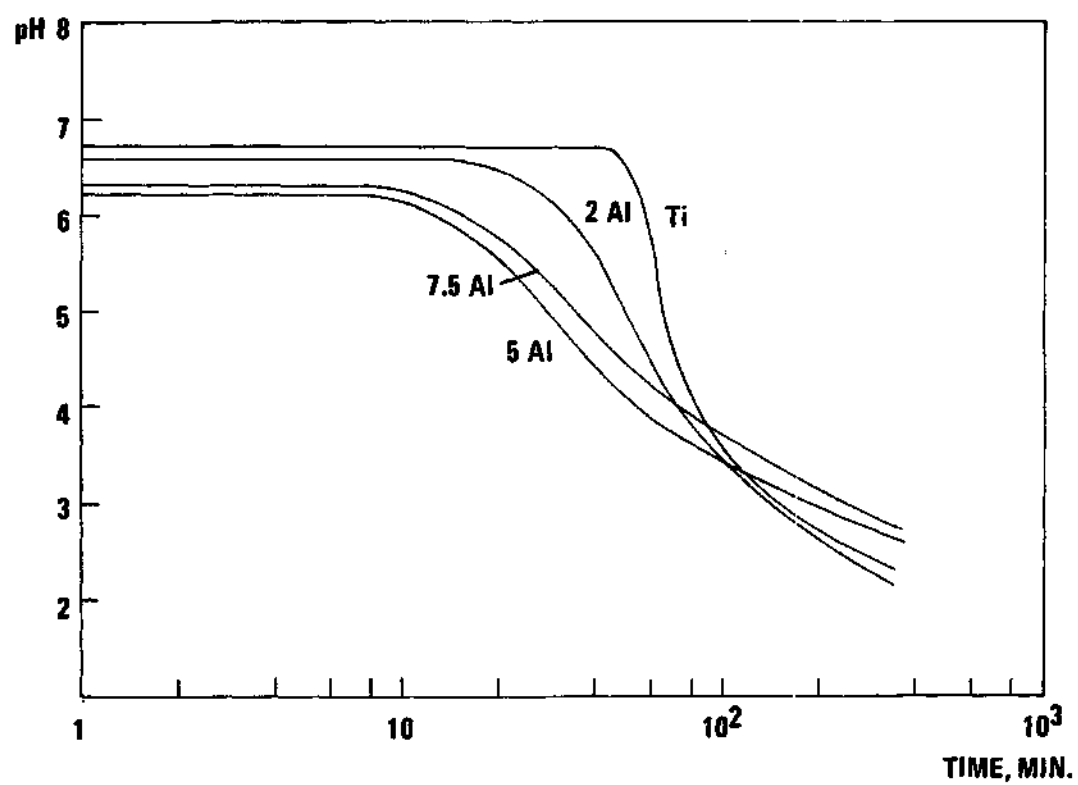


Figure 9. pH-Time Curves for the Materials Tested, Showing Differences in "Incubation" Times



observed in some occasions could be due to the formation of hydrogen peroxide.

The presence of oxygen in solution was proven by tests showing that an amount of about 0.5 ppm of oxygen was still present in the solution after bubbling with nitrogen for 20 minutes. The effect of oxygen was also shown by using non-deaerated solution and keeping it exposed to air during the experiment. This solution showed practically no pH decrease.

The apparent influence of aluminum in decreasing the "incubation" time, as shown in Table 3, is not clear at the present time. However, the observation agrees with the known fact that aluminum promotes hydrogen pickup by the material and increases the SCC susceptibility in titanium alloys. The effect of aluminum ion interaction with oxygen does not seem to be able to explain the very large differences in "incubation" times between pure titanium and its alloys.

In any case the essential factor marking the beginning of the pH decrease is the complete consumption of the oxygen in the solution. The hydrolysis reaction then liberates hydrogen ions in the solution and this process diminishes as the pH lowers, since the equilibrium constant of the reaction is proportional to the pH. At low pH another reaction intervenes; this is the point at which titanium ions become the stable species in the solution, as indicated by the Pourbaix diagram. When this occurs, further liberation of titanium ions into the solution does not have any appreciable effect on the pH.



### Hydrolysis Products

Tests were made to determine the presence of titanium and aluminum ions in solution, using the methods previously described. An attempt was also made to establish the pH value at which each of these ions could first be detected. An exact pH value was not pinpointed; however, the results indicate that aluminum ions were present in the solution at a pH value around 5, while the presence of titanium ions was detected in the pH range of 2.0 to 2.5.

The nature of the titanium oxide produced is not clear; however, the data shows that above pH 2.5 the product must be insoluble, since no titanium ion is detectable in solution. According to Chen, Beck and Fontana<sup>32</sup> the oxides  $TiO$  and  $Ti_2O_3$  may be soluble in acid conditions, so that it seems reasonable to assume that  $TiO_2$  is the oxide produced above pH 2.5.

### Potential Measurements

Initially three different potential measurements were made. Before starting the experiments the corrosion potential of the electrode in the large beaker was measured and was found to be approximately -200 mV (SCE). After the start of the experiment, the potential of the scratched electrode was measured while a connection was maintained between it and the large area electrode. The potential ranged, during scratching, between -450 and -650 mV (SCE). The last measurement was carried out after disconnecting the two electrodes and measuring only the open circuit potential of the scratched electrode; its value was -1,100 mV (SCE).

While the above values concern data obtained at the onset of each experiment, it was noticed that at low pH values they were different. As



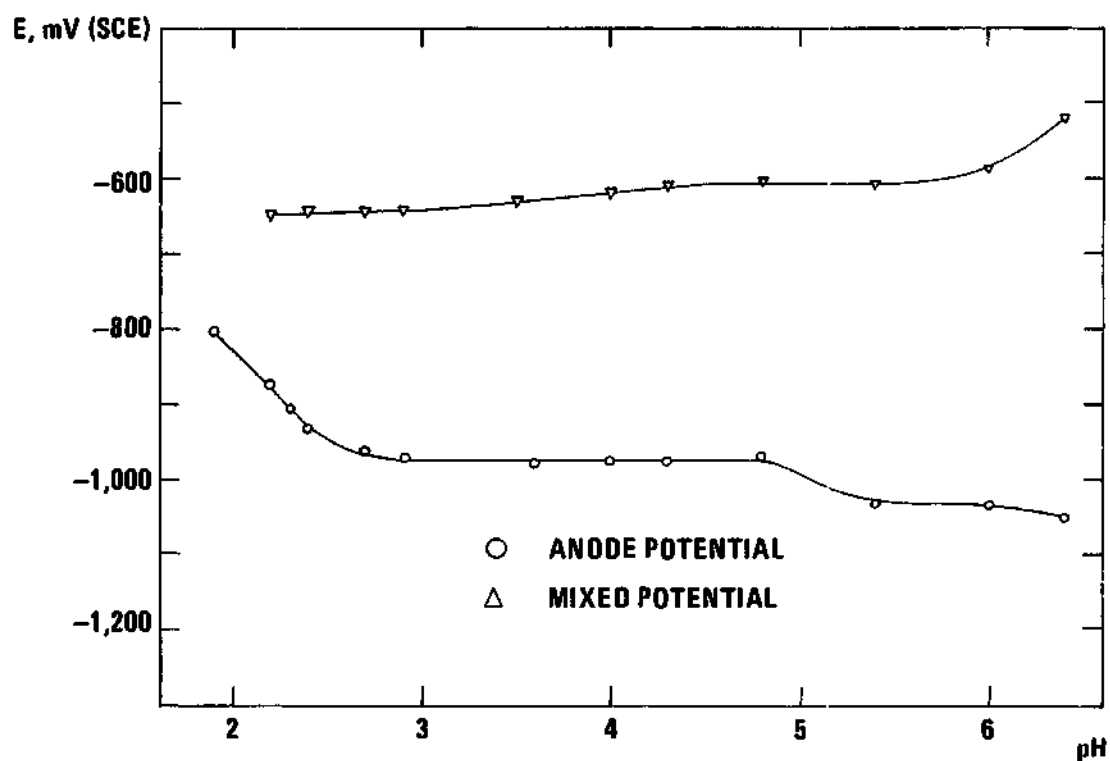


Figure 10. Potential-pH Curves for Pure Titanium, Showing the Effect of pH on Potential.



a result, potential data were recorded while monitoring the pH decrease and potential versus pH curves were obtained. A typical curve, for pure titanium, is shown in Figure 10. It can be seen that the mixed corrosion potential decreases steadily with decreasing pH, with the potential of the scratched electrode undergoing the greatest variation. The values range from -1,100 mV (SCE) at the beginning of the experiments to -800 mV (SCE) at the lowest pH recorded.

To understand these results, it is important to consider the reactions that can occur during the scratching of the specimen, together with their standard potentials; these are shown in Table 4. At the beginning of the test, reactions (1) and (3) occur together with reduction of oxygen, during the "incubation" period. The potential measured inside the small cell during this time is actually the mixed potential of the three reactions. The equilibrium potentials of reactions (1) and (3) are dependent on the pH and this explains the slight increase of the active potential as the pH decreases. According to Beck's model<sup>24</sup> reaction (4) is considered to be the reaction responsible for SCC; in our conditions, however, the rotating diamond tip should remove any previously chemisorbed titanium chloride which, in turn, should hydrolyze to titanium oxide.

Figure 11 is the Pourbaix diagram for pure titanium.<sup>33</sup> The dotted line AB represents the data from Figure 10, where A and B are the initial and final values of pH and potential. It can be seen that the line AB touches the  $\text{Ti}^{++}/\text{TiO}_2$  equilibrium line at about the same pH value at which the active potential undergoes the most marked increase. This confirms the hypothesis that at this point reaction (2) starts to occur



Table 4. Possible Active Surface Reactions and Their Standard Potentials.

Reaction	Potential(SCE)
$\text{Ti} + 2\text{H}_2\text{O} \rightarrow \text{TiO}_2 + 4\text{H}^+ + 4\text{e}$	$E^0 = -1100 \text{ mV} \quad (1)$
$\text{Ti} \rightarrow \text{Ti}^{++} + 2\text{e}$	$E^0 = -1870 \text{ mV} \quad (2)$
$2\text{H}^+ + 2\text{e} \rightarrow \text{H}_2$	$E^0 = -240 \text{ mV} \quad (3)$
$\text{Ti} + m \text{Cl}^- \rightarrow \text{TiCl}_m + m \text{e}$ (chemisorbed)	(4)



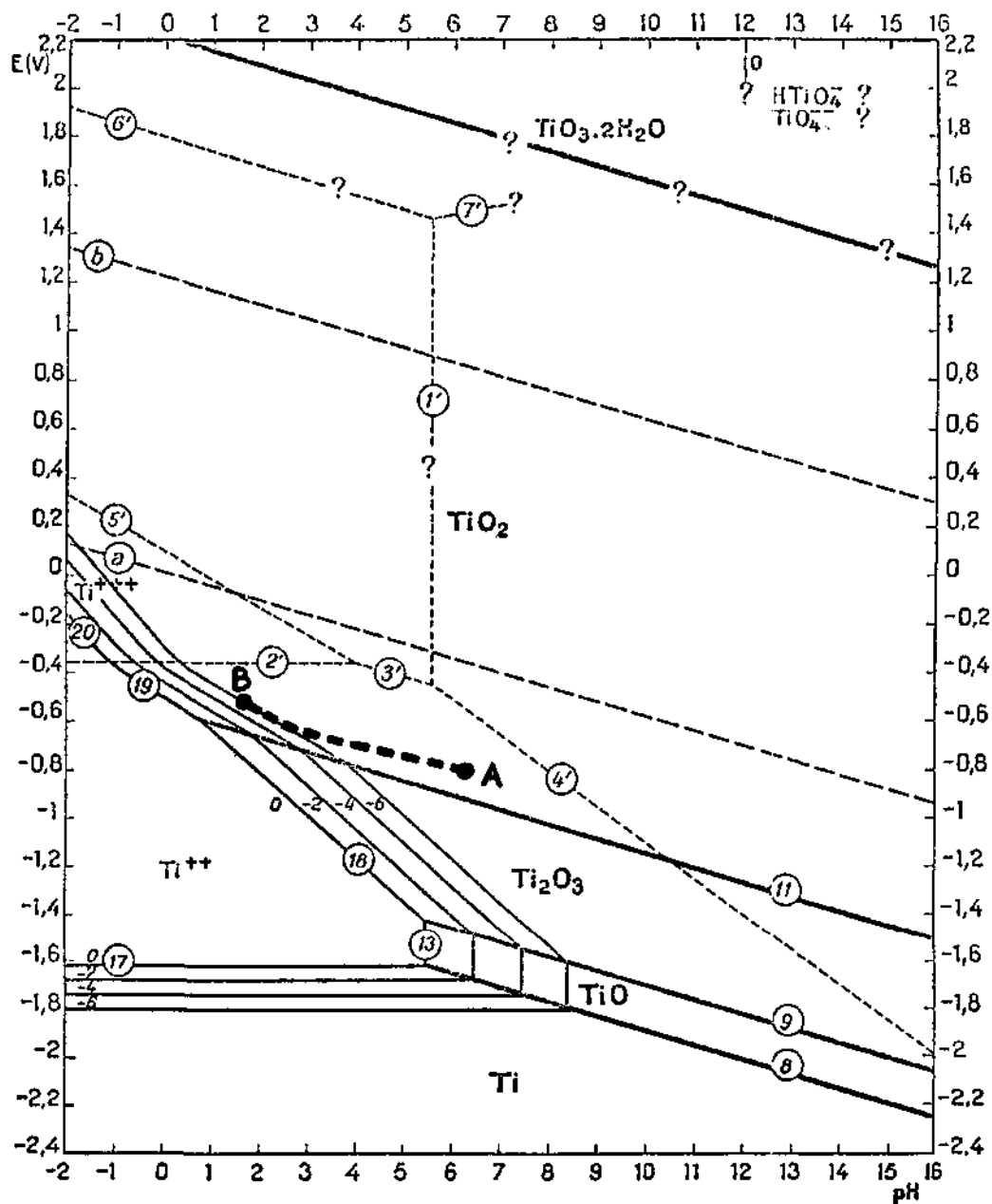


Figure 11. Standard Potential-pH Diagram for Titanium. The Dotted Path AB Shows the Variation of Potential with pH (See Figure 10)



together with reactions (1) and (3). In agreement with this assumption the line AB follows the line of lowest  $Ti^{++}$  concentration.

In applying the pH and potential data to the Pourbaix diagram it must be remembered that disagreement still exists on the accuracy of the diagram of Figure 11. Furthermore the thermodynamic data used in the determination of the diagram are for bulk materials and some correction probably needs to be done when directly relating the data obtained in these experiments.



## CHAPTER IV

## CONCLUSIONS

The conclusions that can be made upon the results of this work are the following:

Potential-Load Experiments

1. The breakdown of the passive film plays an important role in SCC, according to its ability to repair during deformation.
2. Factors that can affect the condition of the film, such as stress relaxation or increase in thickness are also important in SCC.

pH-Time Experiments

1. The increase in acidity at the tip of a stress corrosion crack indicates a form of occluded cell corrosion. The oxygen has a main role in this process, since its removal is essential for the pH decrease. In actual SCC conditions this results from the geometry of the crack.
2. All the materials tested, having a different SCC susceptibility, showed quite similar increases in acidity, both in the rate of the pH decrease and in the final pH values. The observed differences in "incubation" times are not thought to account for the difference in susceptibilities.
3. The pH and potential measurements together with the chemical analysis of the solution indicate that a direct formation of  $TiO_2$  takes place, without the formation of  $TiO$  or  $Ti_2O_3$ .



## CHAPTER V

### RECOMMENDATIONS

1. The experimental set-up used in this research provides a reasonable approximation of the conditions at the tip of a stress corrosion crack and can be utilized in further studies of SCC.

2. Investigations of other localized corrosion phenomena as pitting, crevice corrosion, etc., could also be accomplished. These forms of corrosion do not involve the presence of stress and, since this scratching technique causes deformation in the material, the results should be checked with other methods that minimize or eliminate plastic deformation of the material.

3. The verification of existing Pourbaix diagrams, as well as their determination for alloys, could be attained by point-by-point pH and potential measurements and chemical analysis of the species present in solution.



## BIBLIOGRAPHY

1. R. W. Staehle, Proceedings of Conference, Fundamental Aspects of Stress Corrosion Cracking, Ohio State University (NACE), p. 3 (1969).
2. G. C. Kiefer and W. W. Harple, Metal Progress, 63, 74 (1953).
3. B. F. Brown, ASTM Annual Meeting, Lafayette, Ind., June 13-18 (1965).
4. J. A. Feeney and M. J. Blackburn, The Theory of Stress Corrosion Cracking in Alloys, Brussels (NATO), p. 355 (1971).
5. J. C. Williams, ASM Trans. Quart., 60, 646 (Dec. 1967).
6. D. T. Powell and J. C. Scully, Corrosion, 24, 151 (1968).
7. T. R. Beck, J. Electrochem. Soc., 115, 890 (1968).
8. H. L. Logan, J. of Res., NBS, 48, 99 RP 2291 (1952).
9. A. J. Mc Evily and A. P. Bond, J. Electrochem. Soc., 112, 131 (1965).
10. A. J. Sedriks, P. W. Slattery, and E. N. Pugh, Proceedings of Conference, Fundamental Aspects of Stress Corrosion Cracking, Ohio State University (NACE), p. 673 (1969).
11. N. G. Feige and T. Murphy, Metals Eng. Quart., 7, no. 1, 53 (1967).
12. N. Petch and P. Stables, Nature, 169, 842 (1952).
13. H. H. Uhlig, Physical Metallurgy of Stress Corrosion Fracture, Interscience, p. 1 (1959).
14. E. G. Coleman, D. Weinstein, and W. Rostoker, Acta Met., 9, 491 (1961).
15. H. H. Uhlig and J. Sava, Trans. Am. Soc. Metals, 56, 361 (1963).
16. U. R. Evans, Stress Corrosion Cracking and Embrittlement, Wiley, p. 158 (1956).
17. C. Edeleanu, Ibid., p. 126.
18. D. N. Williams, J. Inst. Metals, 91, 147 (1962-63).
19. H. R. Gray, Proceedings of International Symposium, Stress Corrosion Mechanisms of Titanium Alloys, Georgia Institute of Technology (1971).



20. G. Sanderson and J. C. Scully, Corrosion Sci., 8, 541 (1968).
21. J. C. Scully, Proceedings of International Symposium, Stress Corrosion Mechanisms of Titanium Alloys, Georgia Institute of Technology (1971).
22. T. P. Hoar and J. G. Hines, J. Iron and Steel Inst., 182, 124 (1956).
23. T. P. Hoar, Corrosion, 19, 331t (1963).
24. T. R. Beck, J. Electrochem. Soc., 116, 177 (1969).
25. T. R. Beck, Proceedings of Conference, Fundamental Aspects of Stress Corrosion Cracking, Ohio State University (NACE), p. 605 (1969).
26. B. F. Brown, Corrosion, 26, 249 (1970).
27. T. P. Hoar, Trans. Farad. Soc., 33, 1152 (1937).
28. C. Edeleanu, Physical Metallurgy of Stress Corrosion Fracture, Interscience, p. 223 (1959).
29. B. F. Brown, C. T. Fujii, and E. P. Dahlberg, J. Electrochem. Soc., 116, 218 (1969).
30. B. F. Brown, Proceedings of International Symposium, Stress Corrosion Mechanisms of Titanium Alloys, Georgia Institute of Technology (1971).
31. T. R. Beck, Quarterly Progress Report No. 9, Boeing Scientific Research Laboratories, (1968).
32. C. M. Chen, F. H. Beck, and M. G. Fontana, Proceedings of International Symposium, Stress Corrosion Mechanisms of Titanium Alloys, Georgia Institute of Technology (1971).
33. M. Pourbaix, Atlas of Electrochemical Equilibria in Aqueous Solutions, Pergamon Press, (1966).